NACA

RESEARCH MEMORANDUM

FLIGHT INVESTIGATION OF THE EFFECT OF VERTICAL-TAIL SIZE ON THE ROLLING BEHAVIOR OF A SWEPT-WING AIRPLANE HAVING LATERAL-LONGITUDINAL COUPLING

By Thomas W. Finch, James R. Peele, and
Richard E. Day

High-Speed Flight Station
Edwards, Calif.

NATIONAL ADVISORY COMMITTEE
FOR AERONAUTICS

WASHINGTON

April 10, 1956
Declassified February 10, 1959

NATIONAL ADVISORY COMMITTEE FOR AERONAUTICS

RESEARCH MEMORANDUM

FLIGHT INVESTIGATION OF THE EFFECT OF VERTICAL-TAIL SIZE ON THE ROLLING BEHAVIOR OF A SWEPT-WING AIRPLANE HAVING LATERAL-LONGITUDINAL COUPLING

By Thomas W. Finch, James R. Peele, and
Richard E. Day

SUMMARY

Flight tests have been performed over a Mach number range of 0.73 to 1.39 to determine the rolling behavior of a swept-wing airplane having lateral-longitudinal coupling. The tests were made at altitudes of 40,000 feet and 30,000 feet and employed three different vertical tails with varying aspect ratio or area, or both, and two wing configurations, the basic wing, and the basic wing plus wing-tip extensions.

The airplane with the original vertical tail exhibited violent motions resulting from cross coupling at the higher rolling velocities. Consequently, tests with this configuration were limited to low aileron deflections and to bank angles less than 90°. Doubling the directional stability by increasing the tail area 27 percent and the tail aspect ratio 32 percent greatly improved the rolling behavior enabling rolling rates on the order of 3 to 4 radians per second to be obtained.

The adverse sideslip encountered during roll maneuvers decreased with increasing speeds to negligible values over a Mach number range of approximately 1.00 to 1.05; the sideslip then increased in a favorable direction with further increases in speed. The present allowable sideslip angles imposed by structural limitations were not approached at either subsonic or supersonic speeds. Engine gyroscopic effects caused the rolling behavior to be worse in left rolls at subsonic speeds (adverse yaw) and in right rolls at supersonic speeds (favorable yaw).

Small airplane nose-up stabilizer motion during the roll made the behavior considerably worse at subsonic speeds, whereas small stabilizer motion in the opposite direction improved the behavior. At supersonic speeds the reverse is true, but to a lesser degree.

INTRODUCTION

The possibility of encountering large angles of sideslip or attack, or both, as a result of lateral-longitudinal coupling during rolling maneuvers has been treated theoretically in reference 1. It was concluded that airplanes can encounter lateral and longitudinal divergence in rolling maneuvers if the rate of roll is sufficiently high and the pitch and yaw stability are not properly proportioned. Large angles of sideslip or angles of attack might be expected when the rolling velocity approaches the natural frequency in yaw or pitch.

Violent motions resulting from rolling maneuvers with a straight-wing research airplane and also with the swept-wing airplane discussed in this paper were reported in reference 2. Similar behavior occurring during maneuvers of a delta-wing airplane was reported in reference 3. Since the aerodynamic and mass characteristics of these configurations are representative of current design practice, it may be anticipated that many present and future configurations could encounter the same problem.

Because of the severe roll coupling involved in performing large deflection rolls with the original tail, the rolls with this tail were limited to small bank angles and low aileron deflections, and a program was initiated to study the effect of an increase in vertical-tail size on the rolling behavior.

This paper presents data obtained during the investigation of rolling behavior of a swept-wing fighter-type airplane with three different vertical tails which have been used to establish a progressively higher level of directional stability as reported in reference 4, and with two wing configurations, the basic wing and the basic wing plus wing-tip extensions.

SYMBOLS

A aspect ratio, $\frac{b^2}{S}$

a_n normal acceleration, g units

a_t transverse acceleration, g units

b wing span, ft

C_n yawing-moment coefficient, $\frac{\text{Yawing moment}}{qSb}$

$C_{n_\beta} = \frac{\partial C_n}{\partial \beta}$

c	chord, ft
$\bar{c}$	mean aerodynamic chord, ft
F_a	aileron stick force, lb
F_r	rudder pedal force, lb
F_s	stabilizer stick force, lb
g	acceleration due to gravity, ft/sec^2
h_p	pressure altitude, ft
I_X	moment of inertia about X-axis, slug-ft^2
I_Y	moment of inertia about Y-axis, slug-ft^2
I_Z	moment of inertia about Z-axis, slug-ft^2
I_{XZ}	product of inertia, slug-ft^2
i_t	angle of tail incidence measured from line parallel to longitudinal axis of airplane, deg
M	Mach number
p	rolling angular velocity, radians/sec
q	pitching angular velocity, radians/sec
r	yawing angular velocity, radians/sec
S	wing area, sq ft
t	time, sec
α	indicated angle of attack, deg or radians
β	indicated angle of sideslip, deg

$\Delta\alpha$ increment in angle of attack, deg

$\Delta\beta$ increment in angle of sideslip, deg

δ_a aileron deflection, deg

δ_{a_t} total aileron deflection, deg

δ_r rudder deflection, deg

λ taper ratio

$\Lambda_{c/4}$ angle of sweepback at quarter chord, deg

φ bank angle, deg

Subscripts:

max maximum measured value

0 initial condition

AIRPLANE AND INSTRUMENTATION

The airplane utilized in this investigation is a fighter-type with a single turbojet engine and a low swept wing and tail. A drawing and photograph of the airplane with the original vertical tail A are shown in figures 1 and 2, respectively. The geometric and mass characteristics are given in table I.

The three vertical tails used in the program were characterized by differing areas and aspect ratios as follows:

Tail	Area, sq ft	Aspect ratio
A	33.5	1.13
B	37.3	1.49
C	42.7	1.49

Drawings of the three tails defining the above areas are shown in figure 3. A photograph comparing tails A and C is presented in figure 4. The same rudder was employed for all tails.

An additional configuration was tested with tail C consisting of wing-tip extensions which changed the wing characteristics as follows:

	Area, sq ft	Span, ft	Aspect ratio
Basic wing	376	36.6	3.56
Basic wing plus wing-tip extensions	385	38.6	3.88

Complete stability and control instrumentation was installed for the flight research reported in this paper. The angle of attack, angle of sideslip, airspeed, and altitude were sensed on the nose boom. The Mach numbers presented are based on a preliminary calibration of the airspeed installation and are considered accurate to 0.02 at subsonic speeds and to 0.01 at supersonic speeds. The angle-of-attack and angle-of-sideslip data presented in the time histories are corrected for pitching velocity and yawing velocity, respectively. The bank angle was obtained by integrating rolling velocity.

TESTS

Abrupt rudder-fixed aileron rolls from level flight were performed with three different tail configurations as follows:

Tail	M	h_p, ft	δ_{a_t} (approximate deflection)	φ, deg
A	0.73	30,000	2/3	360
A	0.93, 1.25	40,000	Up to 1/3	90
B	0.73	30,000	Up to 2/3	90 and 360
B	0.78 to 1.30	40,000	Up to 2/3	90 and 360
C	0.73	30,000	Up to full	360
C	0.83 to 1.25	40,000	Up to full	360
C	1.34 and 1.39	40,000	Up to 2/3	360

A limited number of rolls were also made with tail C at $M = 0.73$ and $h_p = 30,000$ feet for one-half to full deflections starting the maneuvers from about 0.7g. Data were obtained for tail C with and without wing-tip extensions. Although the wing-tip extensions add some inertia to the airplane, particularly about the roll axis, the overall effect on the inertia characteristics is negligible.

RESULTS AND DISCUSSION

An example of extreme roll coupling (reported in ref. 2) is given in figure 5 which presents the measured quantities for an abrupt two-thirds-deflection aileron roll with the original vertical tail A at $M = 0.73$ at an altitude of about 32,000 feet. No discussion is given for this figure since the maneuver has been adequately covered in references 5 and 6 in combination with an analysis of its analog simulation.

Because of the violent behavior of the airplane during the roll presented in figure 5, the remaining rolls performed with tail A were limited to small deflections and to bank angles less than 90°. The results obtained in the manner described by figure 6 and shown in figure 7 are presented as variations with the maximum rolling velocity of the maximum initial changes in angle of sideslip $\Delta\beta$ and angle of attack $\Delta\alpha$ encountered during the roll. (Changes in $\Delta\beta$ and $\Delta\alpha$ resulting from the recovery phase of the maneuver are discussed later.) In a right roll, positive $\Delta\beta$ indicates adverse sideslip and negative $\Delta\beta$ indicates favorable sideslip. (The term "favorable" is used to indicate that the direction is opposite to that of adverse.) An analog simulation of the roll (fig. 5) indicated that the first peak of the sideslip trace ($\Delta\beta \approx -20^{\circ}$) occurred at a rolling velocity of about 2.4 radians per second. The remaining rolls with tail A were made at rolling velocities less than 1.5 radians per second with maximum values of $\Delta\beta$ and $\Delta\alpha$ equal to -5° and -2°, respectively.

The results of the investigation with tail B are presented in figure 8 for rolls to bank angles of 360°. The rolls were made with aileron deflections up to two-thirds, resulting in maximum rolling velocities generally on the order to 2 to 3 radians per second. The measured sideslip angles were approaching the temporary restriction imposed by the manufacturer because of structural limitations; therefore no larger rolling velocities were investigated. A maximum value of $\Delta\beta = -20^{\circ}$ was recorded with tail B at $M \approx 0.93$ at 40,000 feet (fig. 9). A value of $\Delta\alpha = -2^{\circ}$ ($\Delta g = 0.5$) occurred during the roll but a total change in α of 9° ($\Delta g = 2.1$) occurred during recovery.

Typical time histories of full-deflection rolls performed with tail C at $M \approx 1.26$ are presented in figure 10 and a summary of all results with tail C is presented in figure 11 for rolls to bank angles of 360°. Rolls were made to full aileron deflection at all Mach numbers except at $M \approx 0.83$ and above $M \approx 1.25$ where the tests were limited because it was felt the sideslip angles were tending to approach the temporary structural limitations restriction of the manufacturer. Rolling velocities reached for the full-deflection rolls were on the order of 3 to 4 radians per second. The data for tail C with the basic-wing configuration and the configuration with wing-tip extensions are presented together, since

the only difference between the two configurations was the slightly lower peak rolling rate which was obtained with the wing-tip extensions. The maximum values of $\Delta\beta$ and $\Delta\alpha$ recorded with tail C were -15.5° and -6°, respectively, and occurred at $M \approx 0.73$ and 30,000 feet for a rolling velocity of 3.65 radians per second.

The results presented in figures 7, 8, and 11 are summarized in figure 12 for Mach numbers of approximately 0.73, 0.93, and 1.25 to show the effect of tail size and roll direction. At each of these Mach numbers it may be seen that, at a given rolling velocity, lower values of $\Delta\beta$ and $\Delta\alpha$ generally resulted as tail size increased. This condition is particularly evident at the higher rolling velocities tested. This effect is attributed to the increase in directional stability, as indicated by the results of the analog study reported in reference 5. It was shown that for an increase from 0.001 to 0.002 in the value of C_{n_β}, values of which are comparable to the measured values for tails A and C (ref. 4), the rolling behavior was considerably improved.

Previous figures have shown that at subsonic speeds the sideslip developed during the roll was in the same direction as the roll, or adverse, whereas, at supersonic speeds the sideslip developed in the favorable direction. This is clearly shown in figure 13 which presents the Mach number variation of values of $\Delta\beta$ encountered in one-half and full-deflection rolls with tail C at an altitude of 40,000 feet. For full-deflection right rolls the value of $\Delta\beta$ varied from about 8° at $M = 0.83$ to -8° at $M \approx 1.26$. For comparable left rolls the value of $\Delta\beta$ varied from about -13.5° at $M \approx 0.93$ to 4.0° at $M \approx 1.26$. It is evident from these maneuvers, performed with essentially no stabilizer movement, that the values of $\Delta\beta$ changed from adverse to favorable near Mach numbers of 1.00 to 1.05.

The temporary sideslip restrictions imposed during the tests reported in this paper and the present allowable sideslip angles, both given by the manufacturer because of structural limitations, are shown in figure 13 for an altitude of 40,000 feet. Neither restriction was approached at subsonic speeds. The temporary restrictions were approached at supersonic speeds; however, only about half the present allowable sideslip angle was reached at supersonic speeds near a Mach number of 1.25. In maneuvers where there was adverse stabilizer movement, as discussed subsequently, larger values of $\Delta\beta$ were measured. These values of 12° at $M = 0.93$ and 8° and -9° at $M \approx 1.26$ are shown in figure 13. The maximum values of $\Delta\beta$ measured at $M \approx 0.73$ and 30,000 feet (fig. 11) were 11.5° and -15.5°.

The effect of roll direction may also be seen in previous figures. At subsonic speeds there are appreciably larger values of $\Delta\beta$ and $\Delta\alpha$ measured in left rolls than in the right rolls at the higher rolling

velocities tested. At supersonic speeds there is less effect from roll direction; however, the rolling behavior is somewhat worse in rolls to the right. Unpublished analog studies indicate a similar effect caused by roll direction. When the engine gyroscopic terms were removed from the equations of motion, the left and right rolls were identical, indicating that this asymmetry is caused by engine gyroscopic effects.

As indicated previously, stabilizer movement during the rolling maneuver could considerably affect the rolling behavior. Unpublished analog studies have shown that pitching velocity produced by the change in stabilizer position during a rolling maneuver has considerable influence on roll coupling. An example of the effect of stabilizer movement is given in figure 14 which presents quantities measured during three full-deflection rolls at $M \approx 0.93$ and at 40,000 feet. For stabilizer movements of about 1° (airplane nose-down), 0°, and -2° (airplane nose-up) during the roll, $\Delta\beta$ values on the order of 1.5°, 5°, and 11.5° were encountered. The stabilizer movement apparently had little effect on the initial change in α, since the values of $\Delta\alpha$ were all about -1°. At supersonic speeds stabilizer movement seems to have a smaller effect but in the opposite direction, which might be attributed to favorable yaw at supersonic speeds.

It should be mentioned that only about one-third inch of stick movement is required per degree of stabilizer movement. Although the use of corrective airplane nose-down stabilizer movement during an aileron roll might be expected to improve rolling behavior at subsonic speeds, this procedure would be an unnatural control movement for the pilot because of the initial decrease in angle of attack and normal acceleration during the roll.

Unpublished analog studies indicate that the initial angle of attack for the roll entry had a considerable effect on the rolling behavior. For $M = 0.70$ at 30,000 feet it was found the values of $\Delta\beta$ and $\Delta\alpha$ were negligible when the initial angle of attack was decreased from 5° (equivalent to 1 g flight) to 1°.

This effect was checked in flight at $M \approx 0.73$ and at 30,000 feet for one-half to full-deflection rolls. The results are summarized in figure 15. In all cases when the initial angle of attack was reduced from about 4° to 2.5°, the values of $\Delta\beta$ and $\Delta\alpha$ decreased. It may be assumed that, for a given rolling velocity, larger values of $\Delta\beta$ and $\Delta\alpha$ would be expected at load factors greater than 1.0g.

The previous discussion has been devoted primarily to the maximum initial changes in α and β resulting from the roll input. It should be pointed out that in some cases with tail C at $M \approx 1.25$ for full-deflection rolls (see fig. 10), positive changes in α as large as 5° (data not presented) closely followed the small initial negative values.

The measured values of $\Delta\beta$ and $\Delta\alpha$ resulting from the roll recovery were generally opposite in direction to the values resulting from the roll input and, except for some instances, were generally no greater in magnitude. Unpublished analog studies indicate the values of $\Delta\beta$ and $\Delta\alpha$ were usually as great during roll recovery as they were during the rolling maneuver. The magnitudes of $\Delta\alpha$ and $\Delta\beta$ encountered during roll recovery are in part directly dependent on the type of roll recovery used by the pilot, since all three controls (aileron, rudder, stabilizer) would be used. It is evident that the pilot would use a different recovery technique from rolls in which large values of $\Delta\beta$ and $\Delta\alpha$ resulted (figs. 5 and 9) than from rolls in which only moderate values resulted.

CONCLUSIONS

From the results obtained during the flight investigation of the rolling behavior of a swept-wing airplane with three different vertical tails it may be concluded that:

1. Doubling the directional stability by increasing the tail area 27 percent and increasing the tail aspect ratio 32 percent greatly alleviated the extreme roll coupling with the original vertical tail enabling rolling rates on the order of 3 to 4 radians per second to be obtained.

2. The adverse sideslip encountered during roll maneuvers decreased with increasing speeds to negligible values near Mach numbers of 1.00 to 1.05. The sideslip then increased in a favorable direction with further increases in speed. The present allowable sideslip angles imposed by structural limitations were not approached at either subsonic or supersonic speeds.

3. Engine gyroscopic effects caused the rolling behavior to be worse in left rolls at subsonic speeds (adverse yaw) and in right rolls at supersonic speeds (favorable yaw).

4. Small airplane nose-up motion during the roll made the behavior considerably worse at subsonic speeds, while small stabilizer motions in the opposite direction improved the behavior. At supersonic speeds the reverse is true, but to a lesser degree.

5. The rolling behavior was somewhat improved when the roll entry was performed at a lower angle of attack for a given speed.

6. The wing-tip extensions had no noticeable effect on rolling behavior other than an expected slight reduction in maximum rolling velocity.

High-Speed Flight Station,
National Advisory Committee for Aeronautics,
Edwards, Calif., December 12, 1955.

REFERENCES

1. Phillips, William H.: Effect of Steady Rolling on Longitudinal and Directional Stability. NACA TN 1627, 1948.

2. NACA High-Speed Flight Station: Flight Experience With Two High-Speed Airplanes Having Violent Lateral-Longitudinal Coupling in Aileron Rolls. NACA RM H55A13, 1955.

3. Sisk, Thomas R., and Andrews, William H.: Flight Experience With a Delta-Wing Airplane Having Violent Lateral-Longitudinal Coupling in Aileron Rolls. NACA RM H55H03, 1955.

4. Drake, Hubert M., Finch, Thomas W., and Peele, James R.: Flight Measurements of Directional Stability to a Mach Number of 1.48 for an Airplane Tested With Three Different Vertical Tail Configurations. NACA RM H55G26, 1955.

5. Gates, Ordway B., Jr., Weil, Joseph, and Woodling, C. H.: Effect of Automatic Stabilization on the Sideslip and Angle-of-Attack Disturbances in Rolling Maneuvers. NACA RM L55E25b, 1955.

6. Weil, Joseph, Gates, Ordway B., Jr., Banner, Richard D., and Kuhl, Albert E.: Flight Experience of Inertia Coupling in Rolling Maneuvers. NACA RM H55E17b, 1955.

TABLE I

PHYSICAL CHARACTERISTICS OF AIRPLANE

	Basic wing	Basic wing plus wing-tip extensions
Wing:		
Airfoil section	NACA 64A007	NACA 64A007
Total area (including aileron and 83.84 sq ft covered by fuselage), sq ft	376.02	385.21
Span, ft	36.58	38.58
Mean aerodynamic chord, ft	11.33	11.16
Root chord, ft	15.86	15.86
Tip chord, ft	4.76	4.15
Taper ratio	0.30	0.262
Aspect ratio	3.56	3.86
Sweep at 0.25 chord line, deg	45	45
Incidence, deg	0	0
Dihedral, deg	0	0
Geometric twist, deg	0	0
Aileron:		
Area rearward of hinge line (each), sq ft	19.32	19.32
Span at hinge line (each), ft	7.81	7.81
Chord rearward of hinge line, percent wing chord	25	25
Travel (each), deg	±15	±15
Leading-edge slat:		
Span, equivalent, ft	12.71	12.71
Segments	5	5
Spanwise location, inboard end, percent wing semispan	24.6	23.3
Spanwise location, outboard end, percent wing semispan	94.1	89.2
Ratio of slat chord to wing chord (parallel to fuselage reference line), percent	20	20
Rotation, maximum, deg	15	15
Horizontal tail:		
Airfoil section		NACA 65A003.5
Total area (including 31.65 sq ft covered by fuselage), sq ft		98.86
Span, ft		18.72
Mean aerodynamic chord, ft		5.83
Root chord, ft		8.14
Tip chord, ft		2.46
Taper ratio		0.30
Aspect ratio		3.54
Sweep at 0.25 chord line, deg		45
Dihedral, deg		0
Travel, leading edge up, deg		5
Travel, leading edge down, deg		25
Irreversible hydraulic boost and artificial feel		

TABLE I.- Concluded

PHYSICAL CHARACTERISTICS OF AIRPLANE

	A	B	C
Vertical tail:			
Airfoil section	NACA 65A003.5	NACA 65A003.5	NACA 65A003.5
Area (excluding dorsal fin and area blanketed by fuselage), sq ft	33.5	37.3	42.7
Area blanketed by fuselage (area between fuselage contour line and line parallel to fuselage reference line through intersections of leading edge of vertical tail and fuselage contour line)	2.11	2.11	2.45
Span (unblanketed), ft	6.14	7.45	7.93
Mean aerodynamic chord, ft	5.83	5.51	5.90
Root chord, ft	7.75	7.75	8.28
Tip chord, ft	3.32	2.32	2.49
Taper ratio	0.428	0.301	0.301
Aspect ratio	1.13	1.49	1.49
Sweep at 0.25 chord line, deg	45	45	45
Rudder:			
Area, rearward of hinge line, sq ft	6.3	6.3	6.3
Span at hinge line, ft	3.33	3.33	3.33
Root chord, ft	2.27	2.27	2.27
Tip chord, ft	1.50	1.50	1.50
Travel, deg	±20	±20	±20
Spanwise location, inboard end, percent vertical tail span	4.5	3.7	3.1
Spanwise location, outboard end, percent vertical tail span	58.2	48.0	44.8
Chord, percent vertical tail chord	30.0	30.0	28.4
Aerodynamic balance	Overhanging, unsealed	Overhanging, unsealed	Overhanging, unsealed
Fuselage:			
Length (afterburner nozzle closed), ft			45.64
Maximum width, ft			5.58
Maximum depth over canopy, ft			6.37
Side area (total), sq ft			230.92
Fineness ratio (afterburner nozzle closed)			7.86
Speed brake:			
Surface area, sq ft			14.14
Maximum deflection, deg			50
Power plant:			
Turbojet engine	One Pratt and Whitney J57-P7 with afterburner		
Thrust (guarantee sea level), afterburner, lb			15,000
Military, lb			9,220
Normal, lb			8,000
Airplane weight, lb:			
Basic (without fuel, oil, water, pilot)			19,662
Total (full fuel, oil, water, pilot)			24,800
Center-of-gravity location, percent $\bar{c}$:			
Total weight - gear down			31.80
Total weight - gear up			31.80
Moments of inertia (estimated total weight):			
I_X, slug-ft^2			11,103
I_Y, slug-ft^2			59,248
I_Z, slug-ft^2			67,279
I_{XZ}, slug-ft^2			941
Inclination of principal axis (estimated total weight):			
Below reference axis at nose, deg			0.8

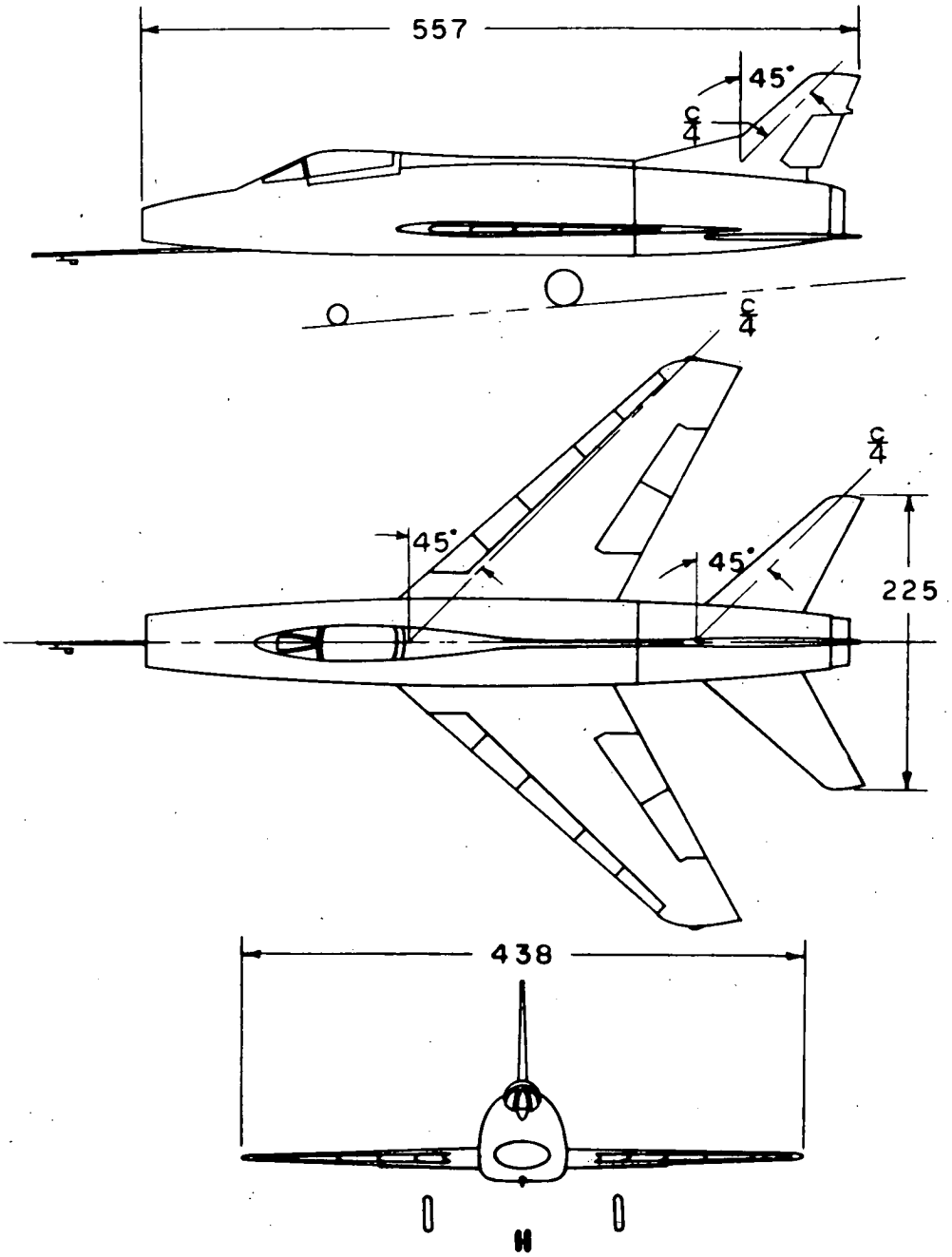

Figure 1.- Three-view drawing of airplane with vertical tail A. All dimensions in inches.

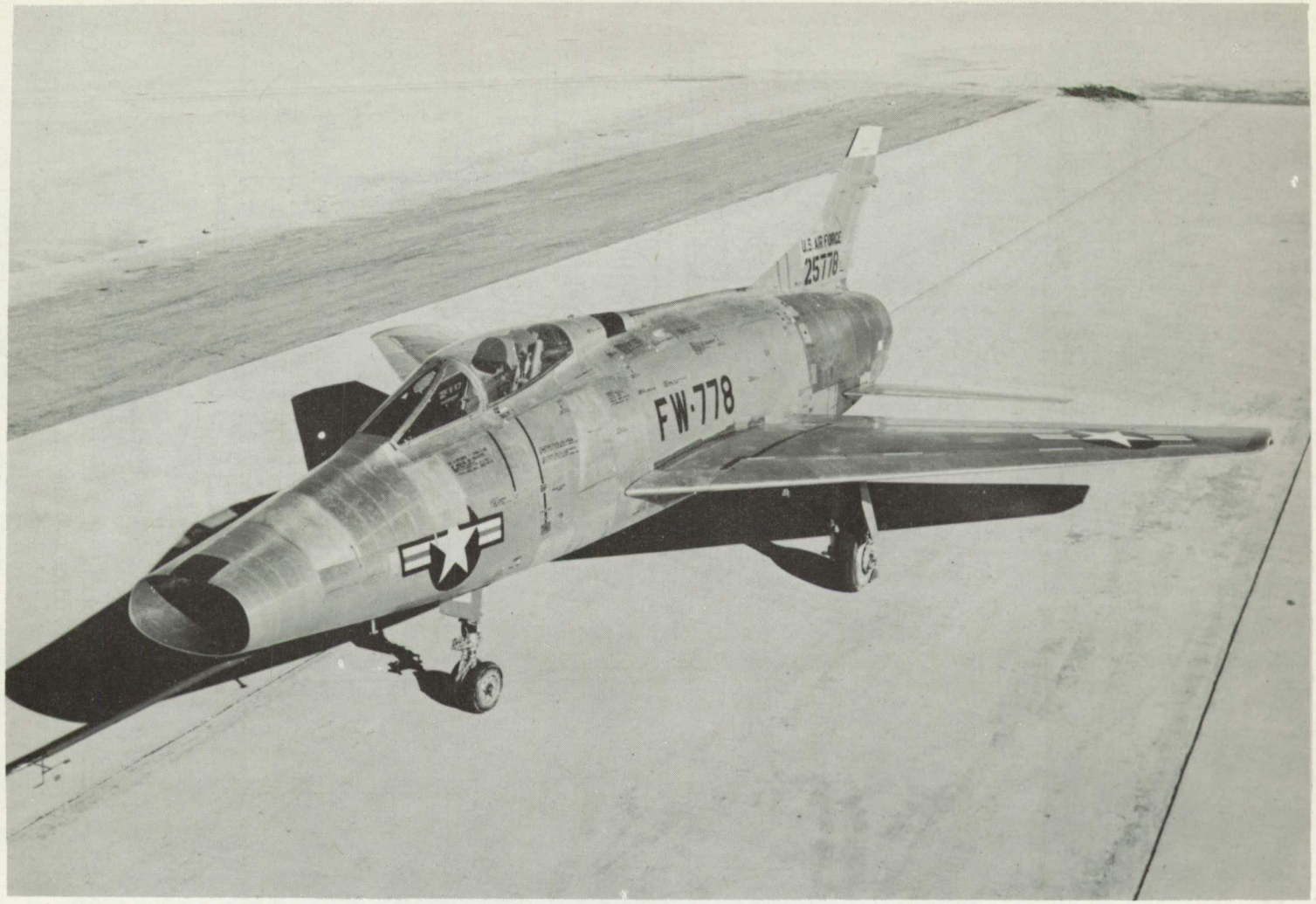

Figure 2.- Photograph of the airplane.

L-91695

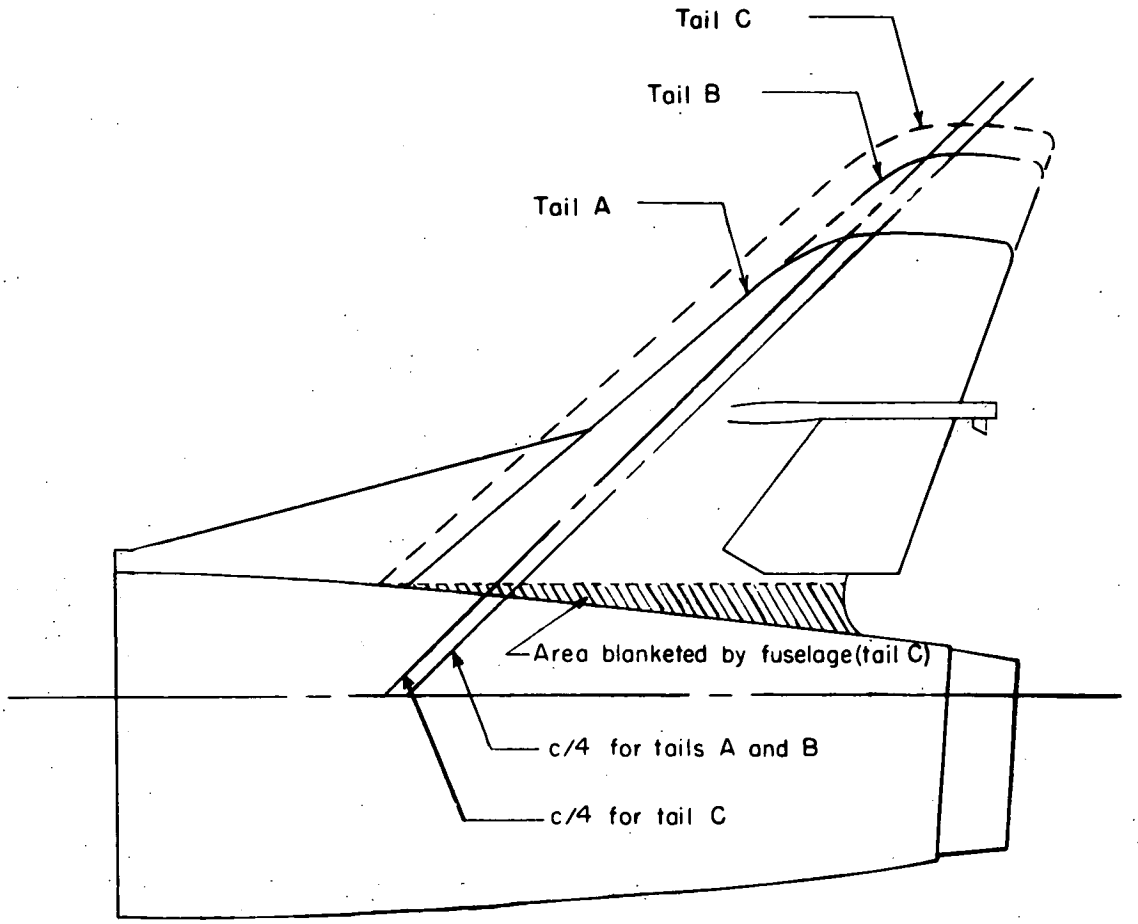

Tail	$\Lambda_{c/4}$, deg	A	λ	Area, sq ft (1)	Span, ft (2)	Blanketed area, sq ft
A	45°	1.13	0.428	33.5	6.14	2.11
B	45°	1.49	0.301	37.3	7.45	2.11
C	45°	1.49	0.301	42.7	7.93	2.45

(1) Area not blanketed by fuselage

(2) Span not blanketed by fuselage

Figure 3.- Sketch of vertical tails A, B, and C.

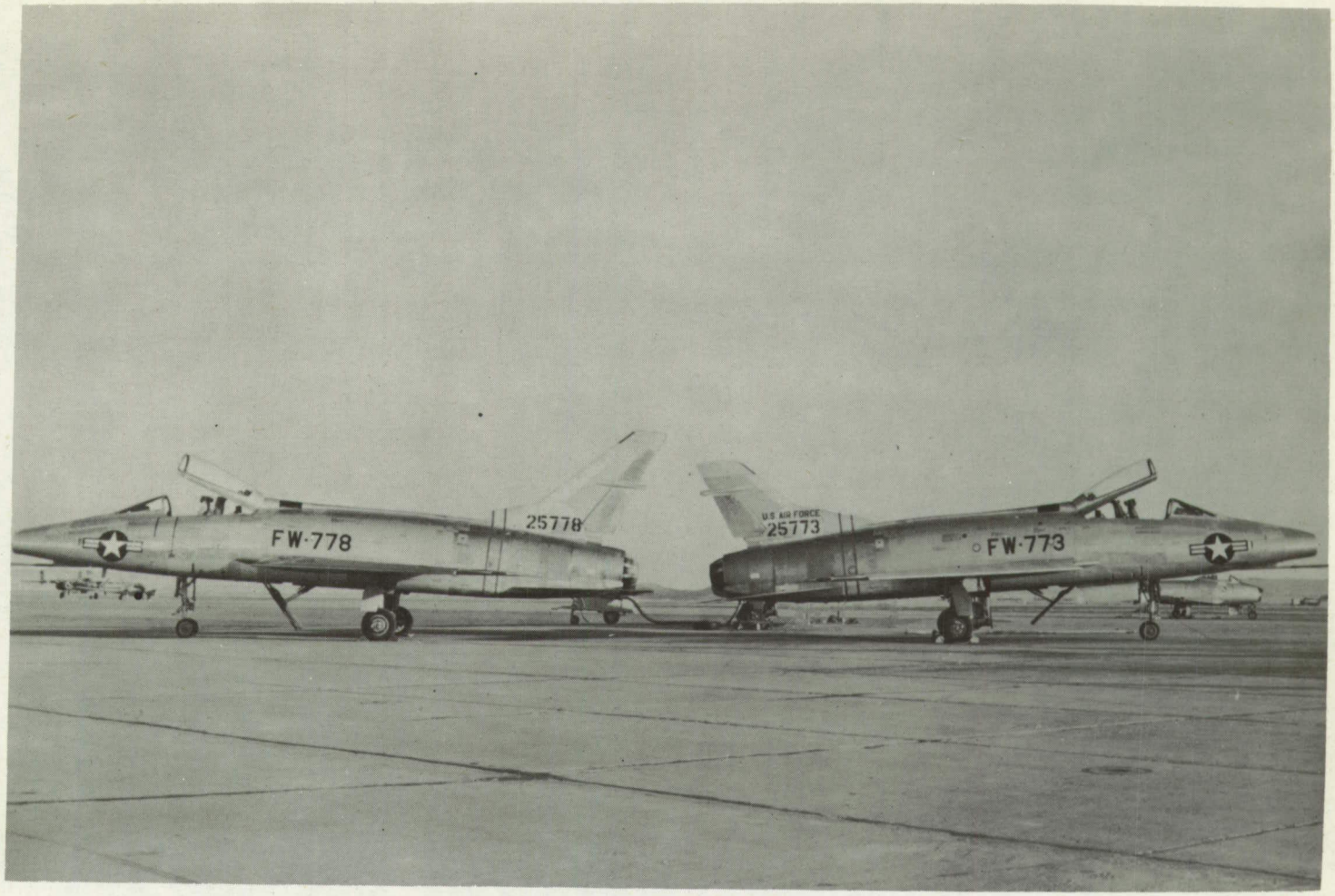

Figure 4.- Photograph of two airplanes showing tails A and C. L-91696

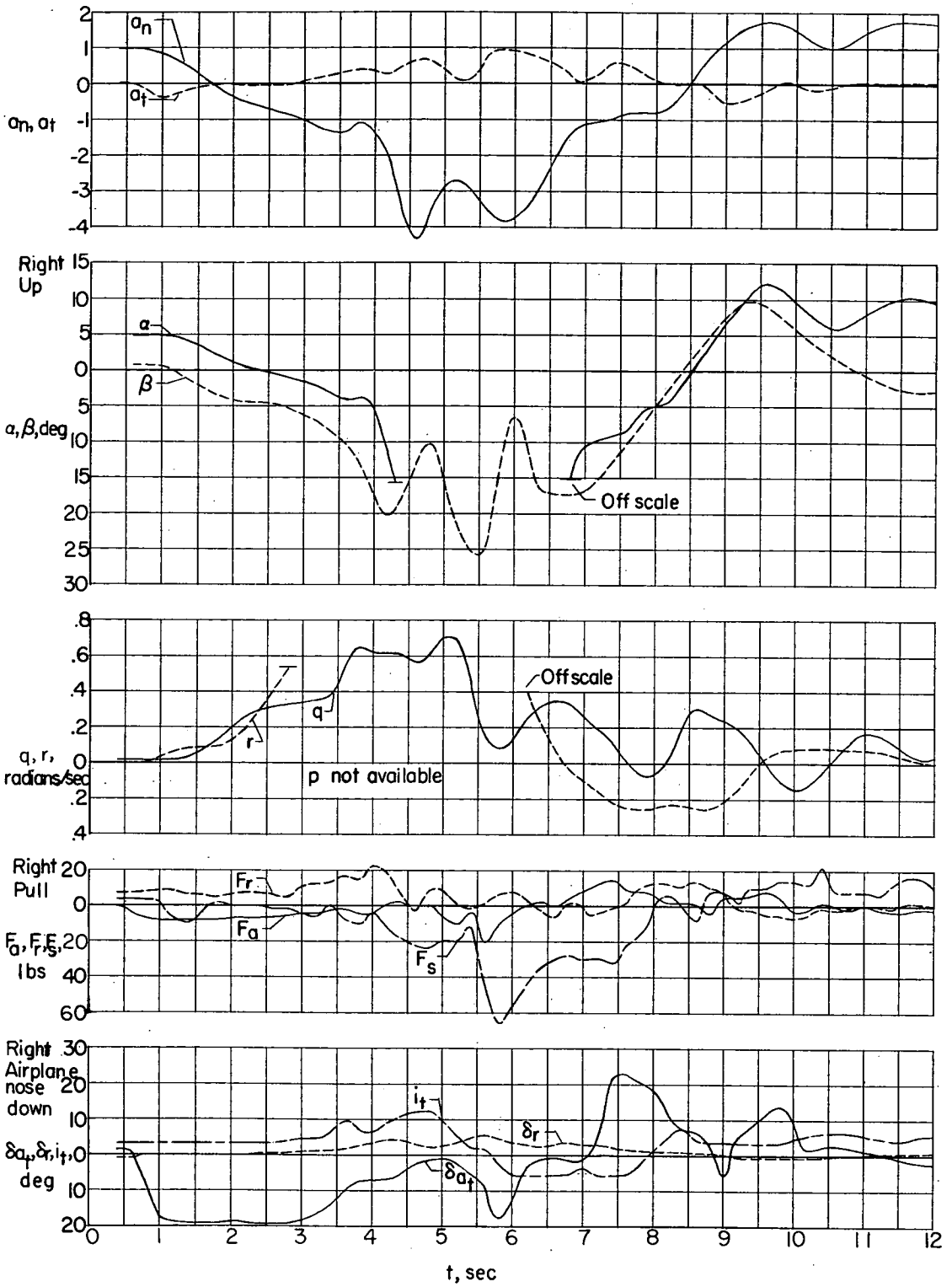

Figure 5.- Quantities measured during a left aileron roll with tail A at $M = 0.73$; $h_p = 33{,}000$ feet.

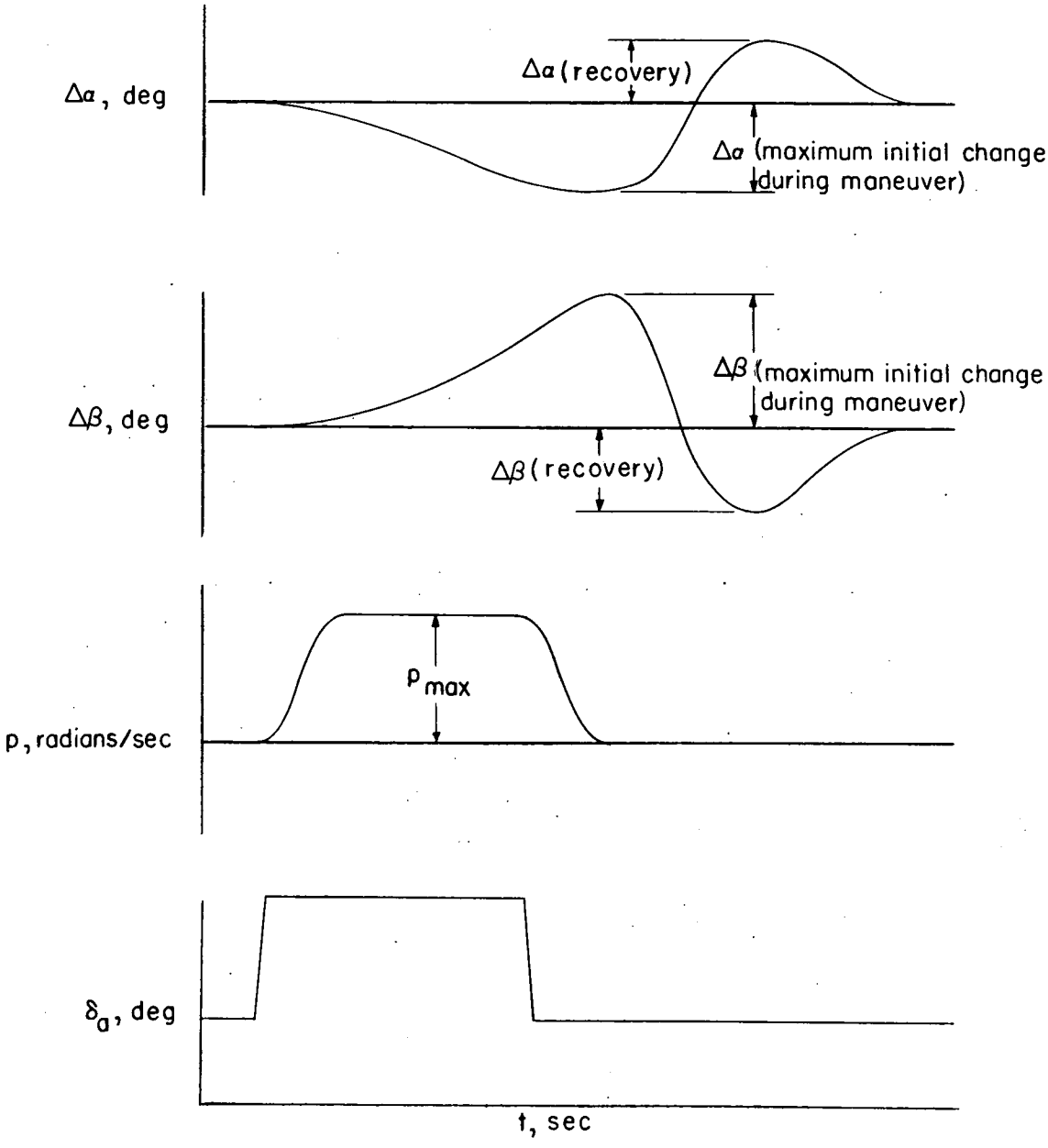

Figure 6.- Sketch of typical roll maneuver showing changes in angles of attack and sideslip.

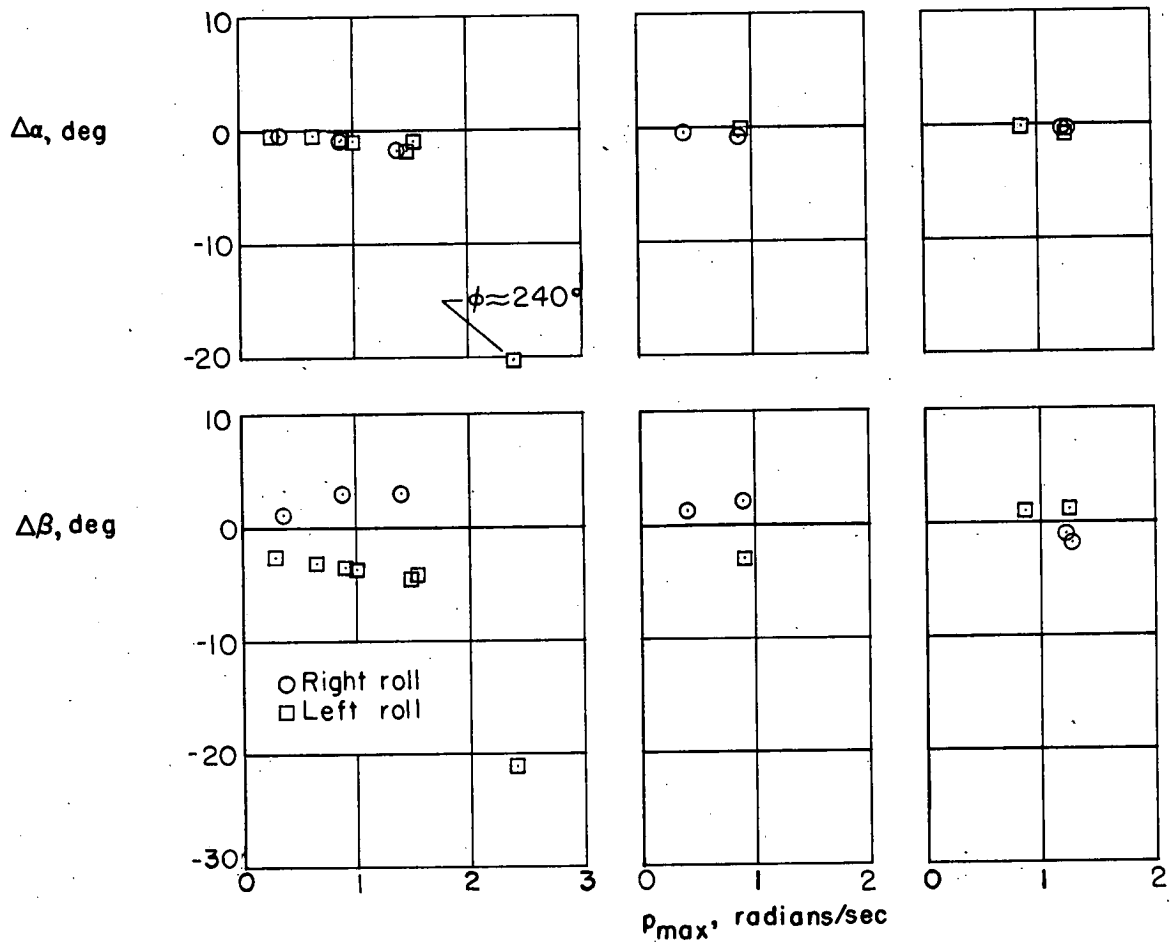

(a) $M \approx 0.73$; $h_p \approx 30{,}000$ feet.

(b) $M \approx 0.93$; $h_p \approx 40{,}000$ feet.

(c) $M \approx 1.25$; $h_p \approx 40{,}000$ feet.

Figure 7.- Variation with maximum rolling velocity of changes in angle of attack and sideslip developed during aileron rolls with tail A for bank angles less than 90°.

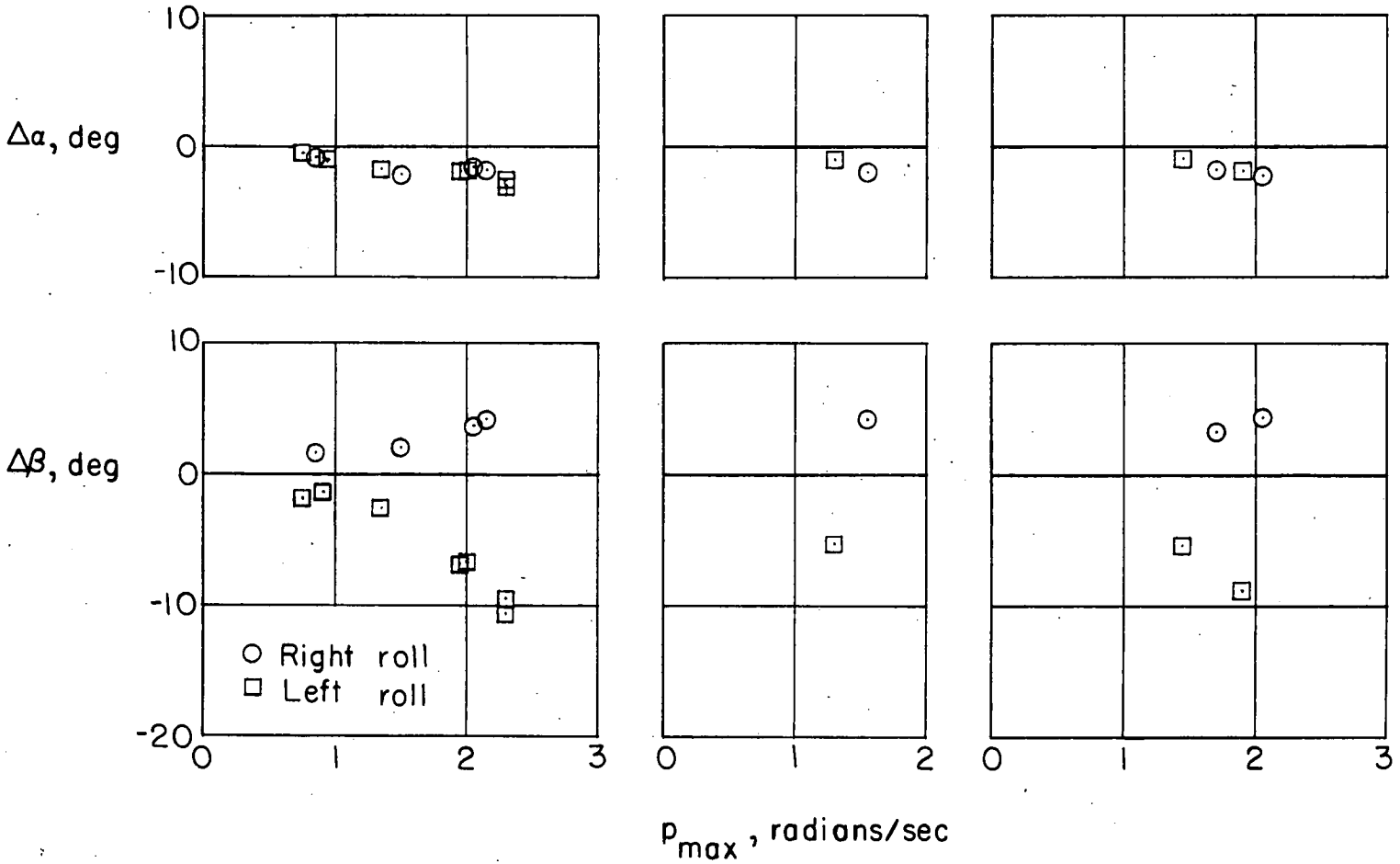

(a) $M \approx 0.73$; $h_p \approx 30{,}000$ feet.

(b) $M \approx 0.78$; $h_p \approx 40{,}000$ feet.

(c) $M \approx 0.83$; $h_p \approx 40{,}000$ feet.

Figure 8.- Variation with maximum rolling velocity of changes in angle of attack and angle of sideslip developed during aileron rolls with tail B for bank angles of 360°.

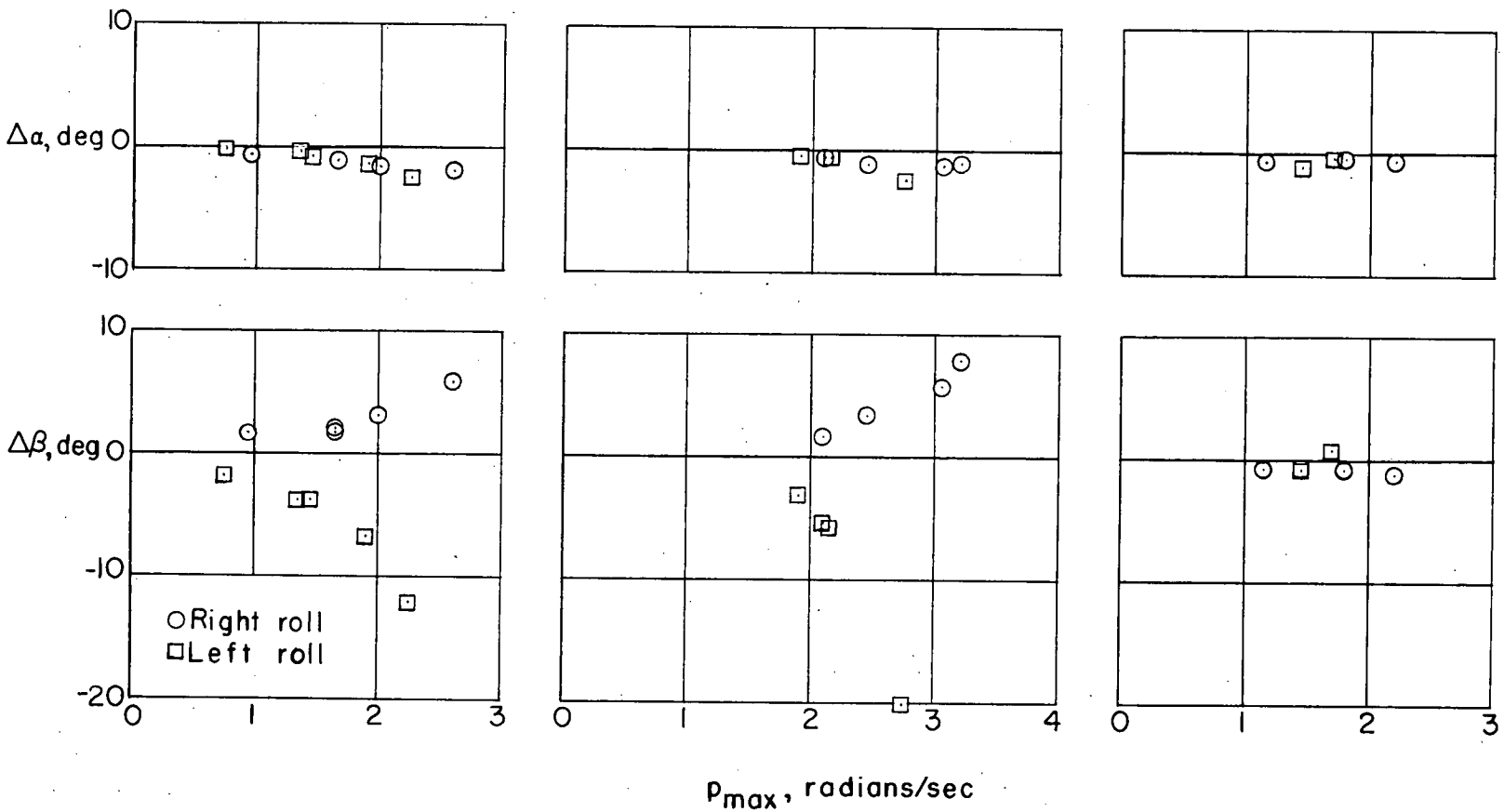

(d) $M \approx 0.88$;
$h_p \approx 40{,}000$ feet.

(e) $M \approx 0.93$;
$h_p \approx 40{,}000$ feet.

(f) $M \approx 1.00$;
$h_p \approx 40{,}000$ feet.

Figure 8.- Continued.

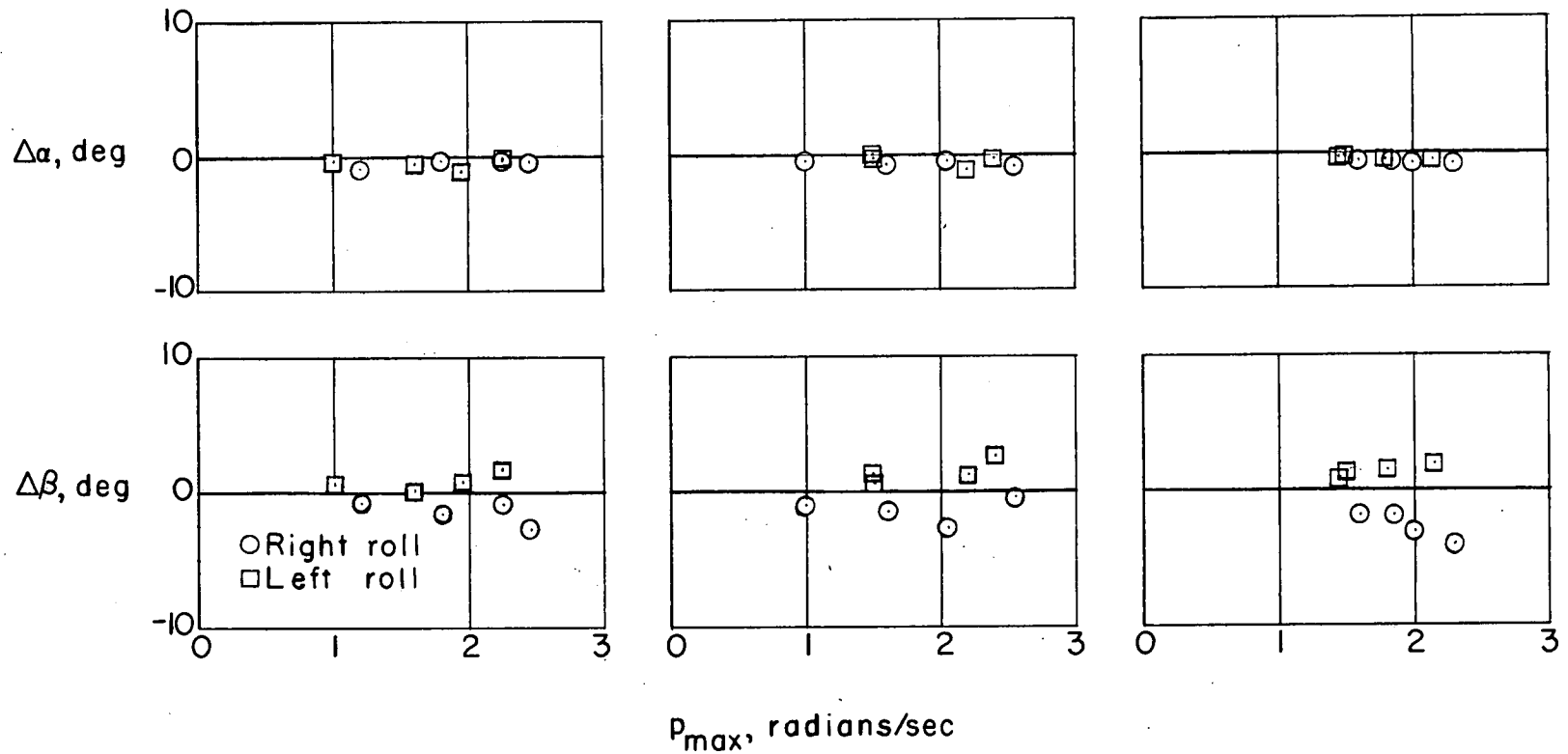

(g) $M \approx 1.05$;
$h_p \approx 40{,}000$ feet.

(h) $M \approx 1.10$;
$h_p \approx 40{,}000$ feet.

(i) $M \approx 1.15$;
$h_p \approx 40{,}000$ feet.

Figure 8.- Continued.

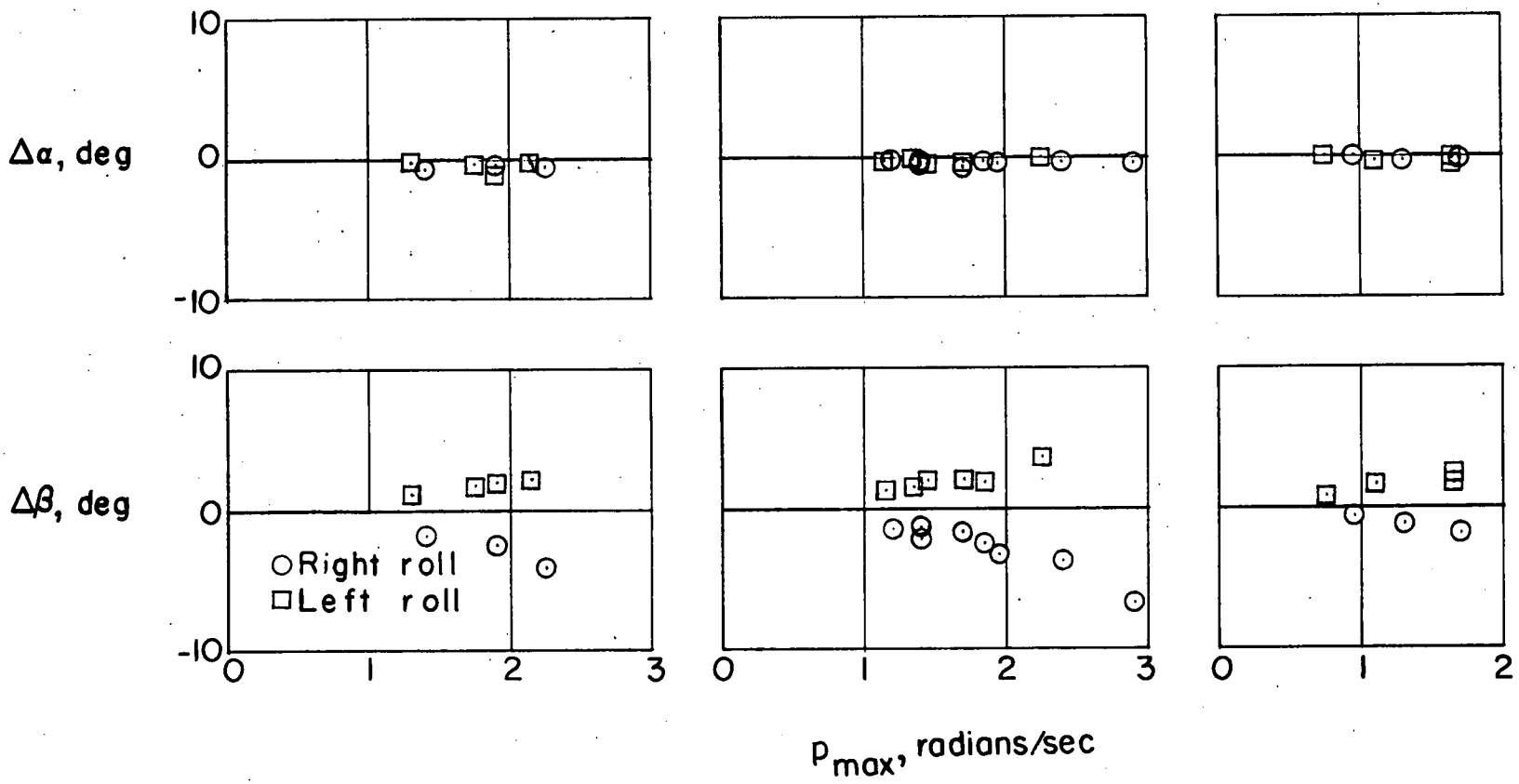

(j) $M \approx 1.20$;
$h_p \approx 40{,}000$ feet.

(k) $M \approx 1.25$;
$h_p \approx 40{,}000$ feet.

(l) $M \approx 1.30$;
$h_p \approx 40{,}000$ feet.

Figure 8.- Concluded.

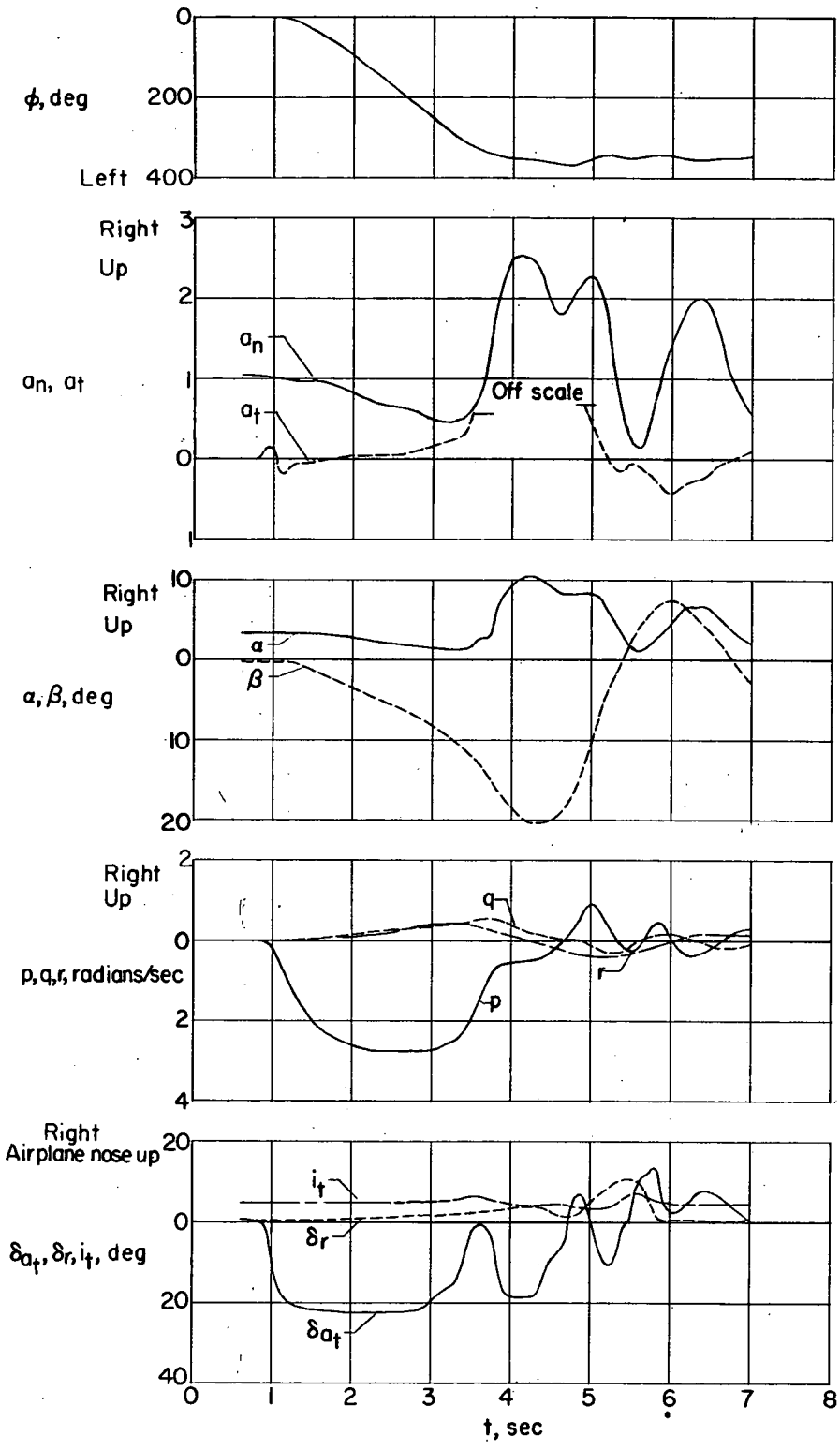

Figure 9.- Quantities measured during a left aileron roll with tail B at $M \approx 0.93$; $h_p = 40{,}000$ feet.

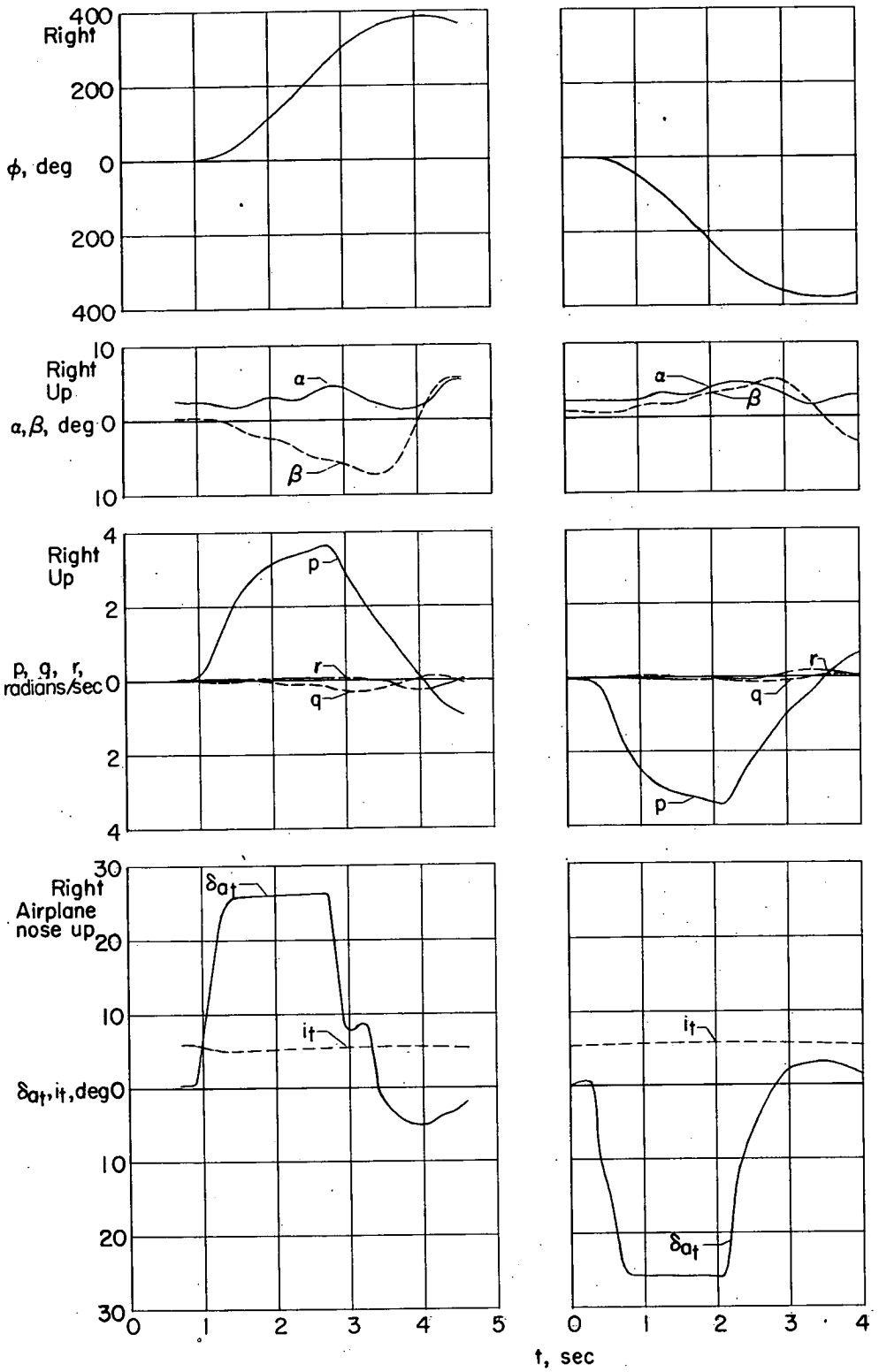

Figure 10.- Quantities measured during full-deflection aileron rolls with tail C at $M \approx 1.26$; $h_p \approx 40{,}000$ feet.

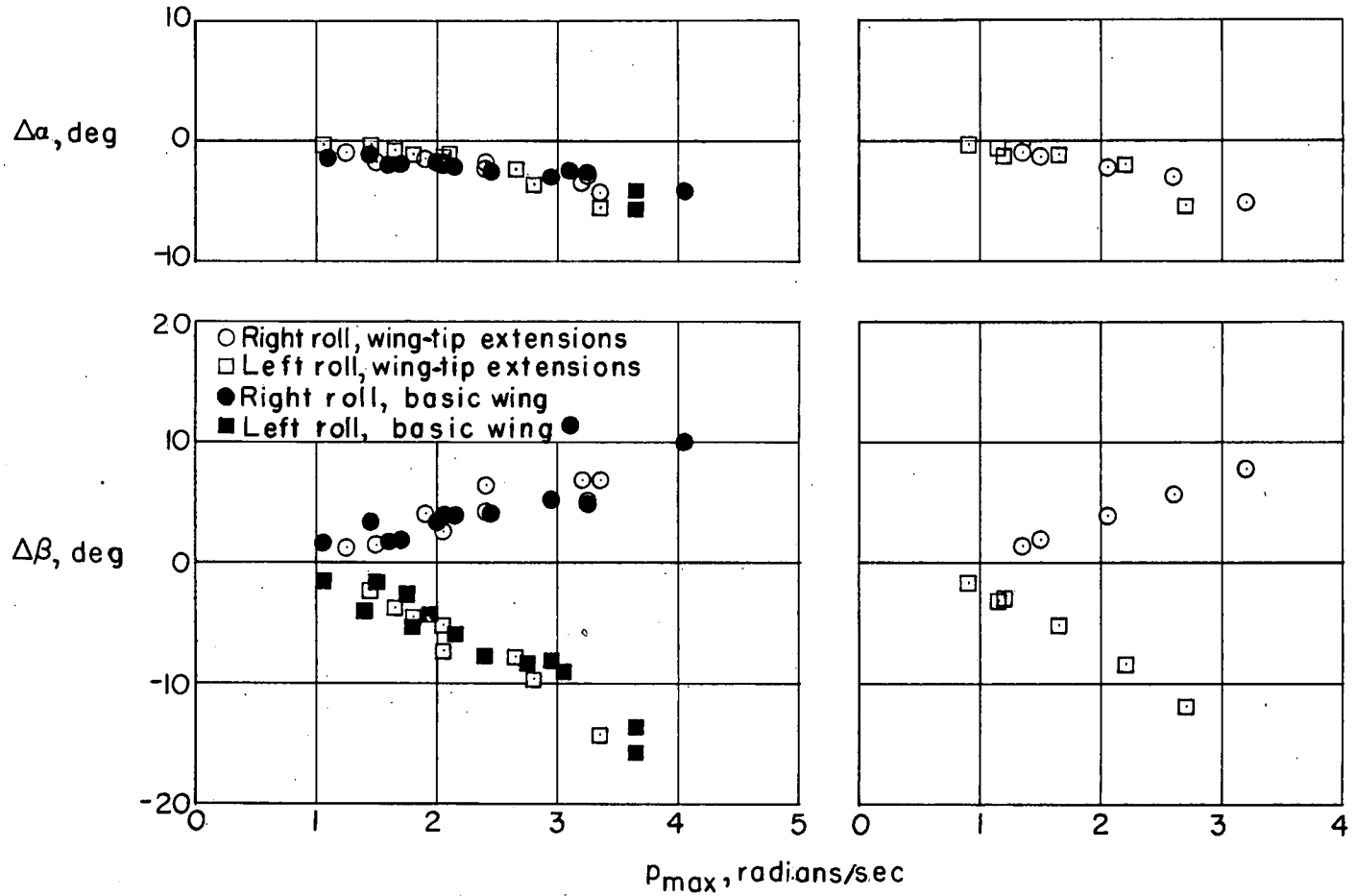

(a) $M \approx 0.73$; $h_p \approx 30{,}000$ feet.

(b) $M \approx 0.83$; $h_p \approx 40{,}000$ feet.

Figure 11.- Variation with maximum rolling velocity of changes in angle of attack and angle of sideslip developed during aileron rolls with tail C.

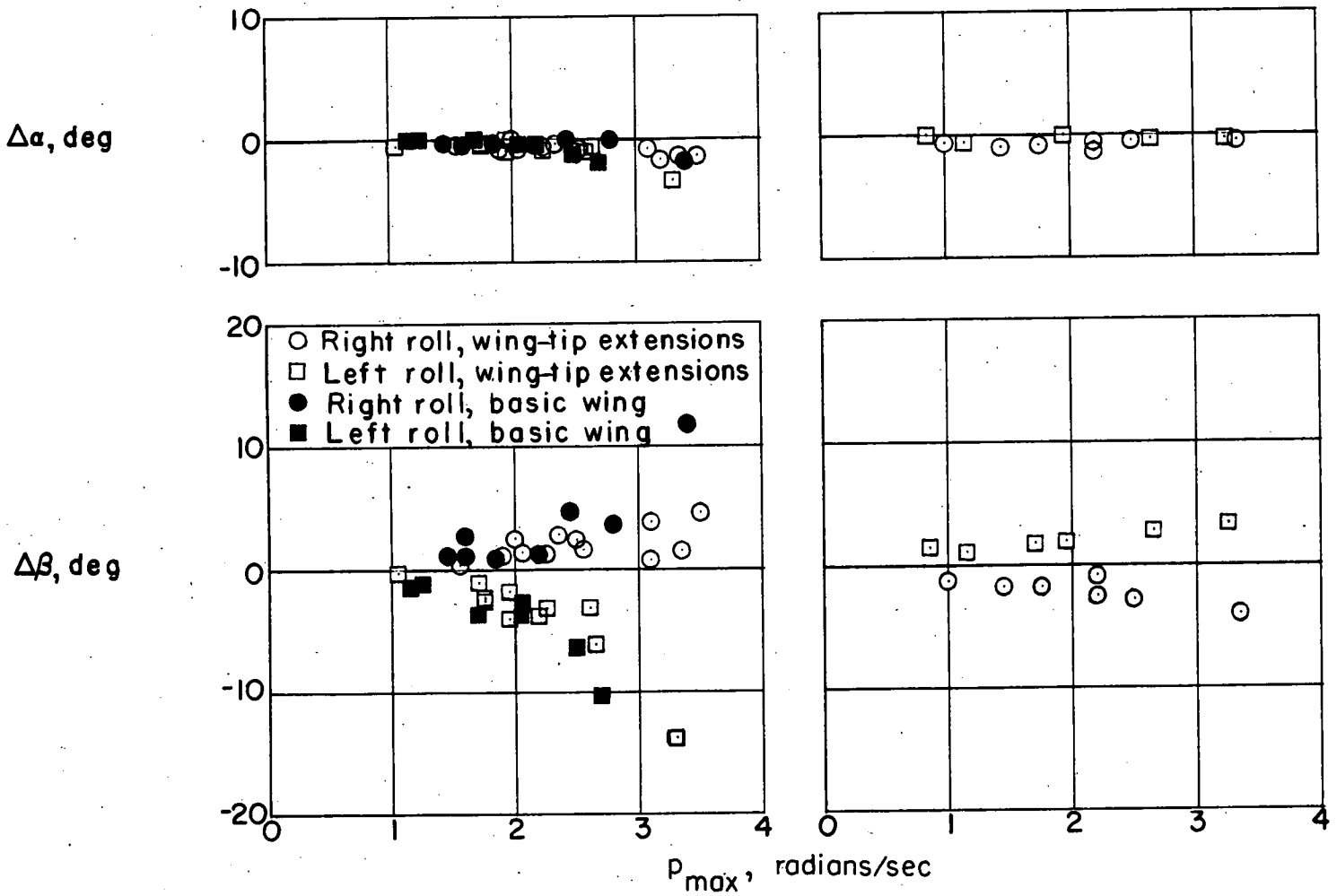

(c) $M \approx 0.93$; $h_p \approx 40{,}000$ feet.

(d) $M \approx 1.15$; $h_p \approx 40{,}000$ feet.

Figure 11.- Continued.

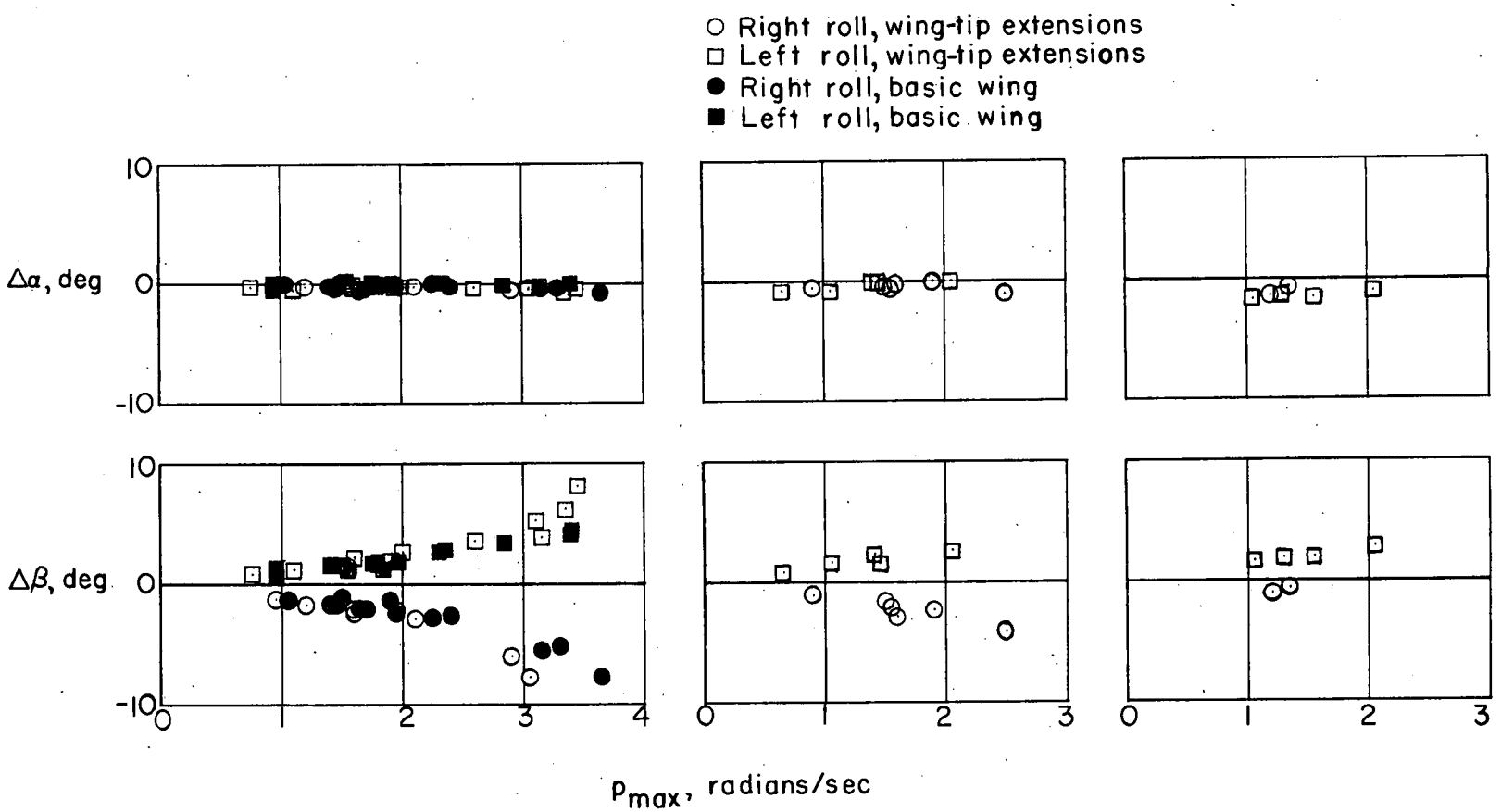

(e) $M \approx 1.25$; $h_p \approx 40{,}000$ feet.

(f) $M \approx 1.39$; $h_p \approx 40{,}000$ feet.

(g) $M \approx 1.39$; $h_p \approx 40{,}000$ feet.

Figure 11.- Concluded.

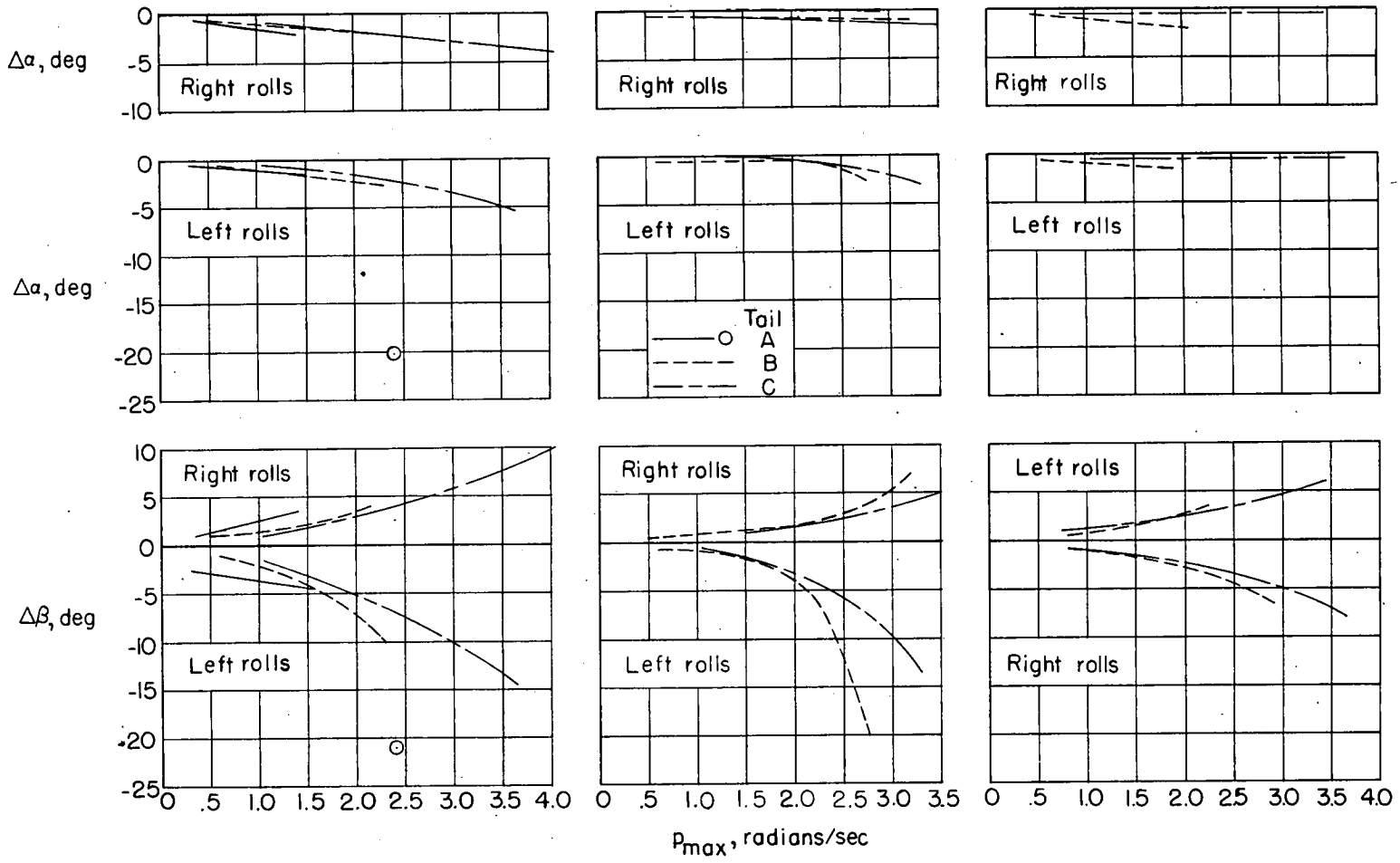

(a) $M \approx 0.73$; $h_p \approx 30{,}000$ feet.

(b) $M \approx 0.93$; $h_p \approx 40{,}000$ feet.

(c) $M \approx 1.25$; $h_p \approx 40{,}000$ feet.

Figure 12.- Effect of tail size and roll direction at several Mach numbers.

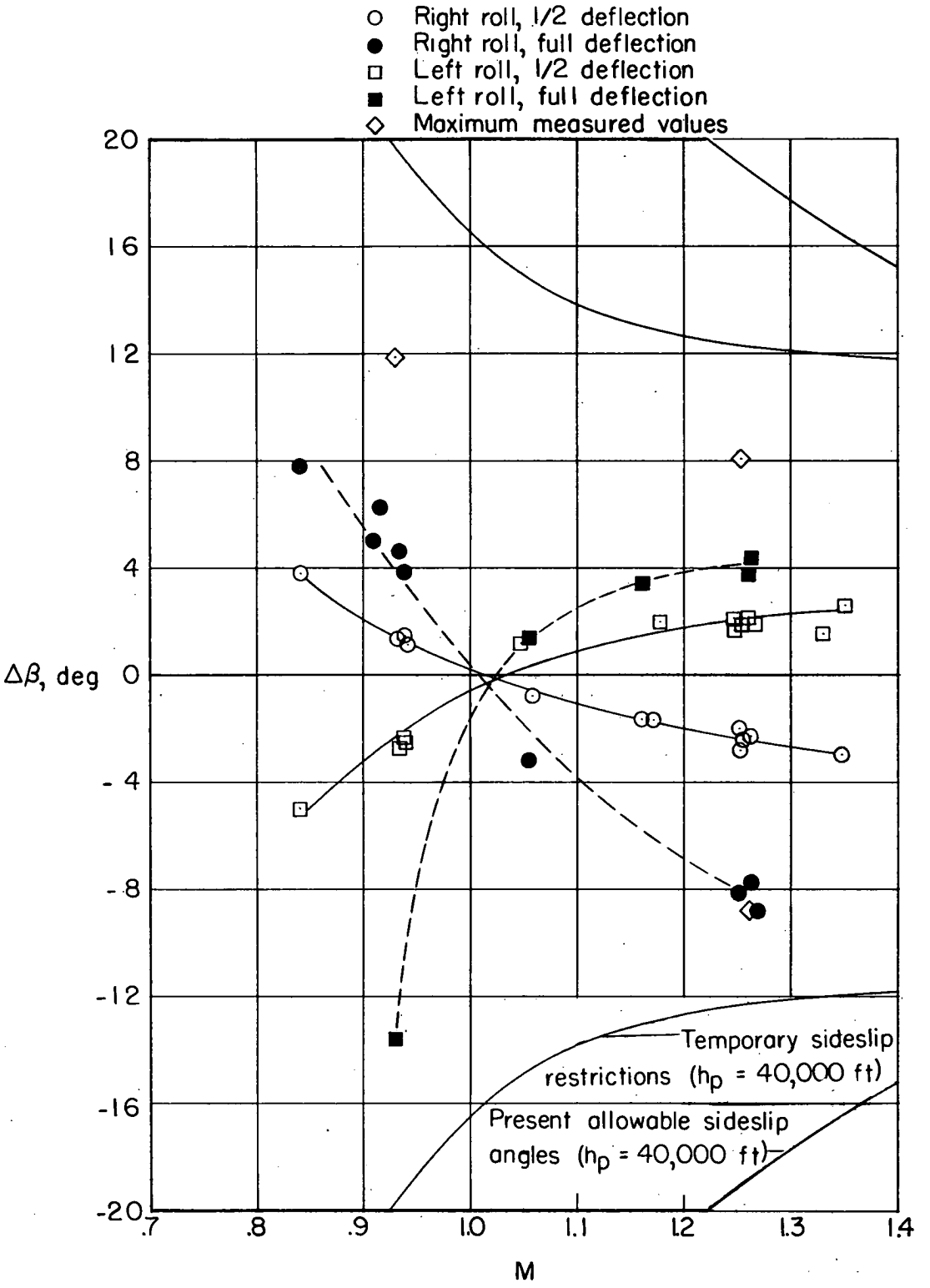

Figure 13.- Effect of Mach number on sideslip angles developed during rolls with essentially no stabilizer motion. Tail C. $h_p \approx 40,000$ feet.

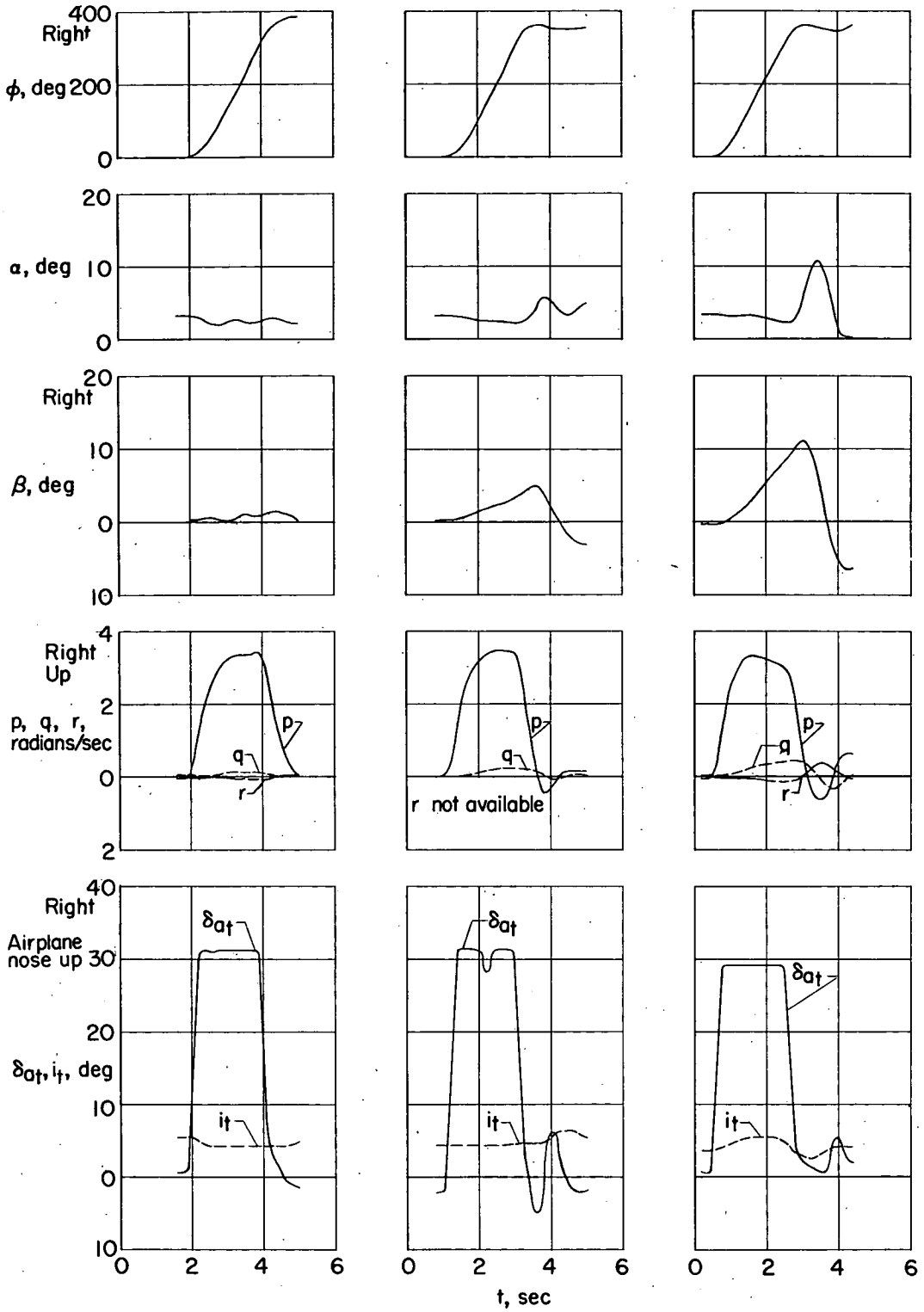

Figure 14.- Effect of stabilizer movement on the rolling motion with tail C at $M \approx 0.93$; $h_p \approx 40,000$ feet.

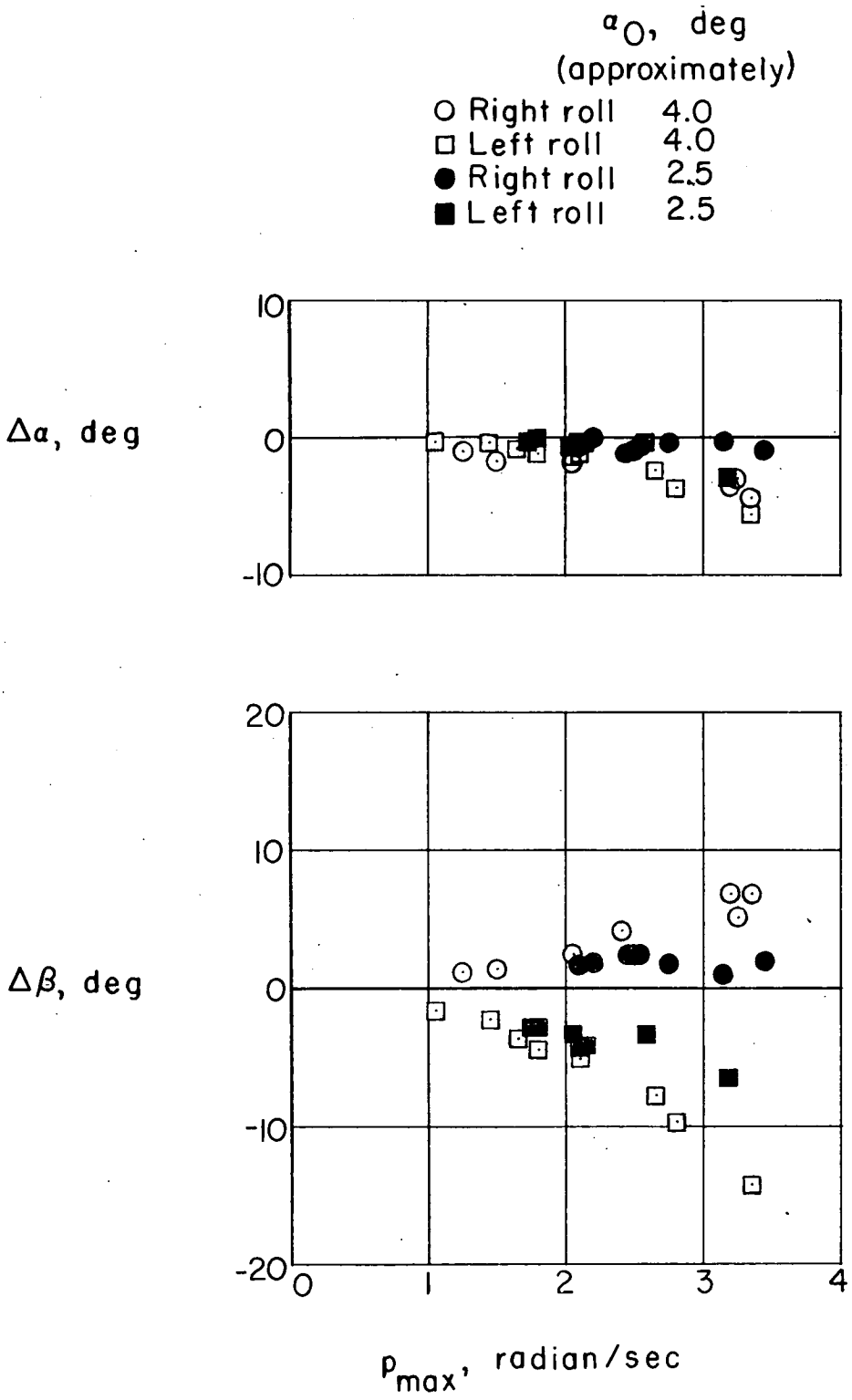

Figure 15.- Effect of angle of attack for roll entry on rolling motion with tail C at $M \approx 0.73$; $h_p \approx 30{,}000$ feet.